DOE/PC/90526--10

DE89 010050

PARTIAL OXIDATION OF LIGHT ALKANES IN TRANSITION METAL ION CONTAINING ZEOLITES

Quarterly Technical Progress Report

for the Period
December 15, 1988-March 14, 1989

Kamil Klier, Jean-Paul Lange, and Richard G. Herman

Zettlemoyer Center for Surface Studies
and
Department of Chemistry
Lehigh University
Bethlehem, PA 18015

April 1989

PREPARED FOR THE UNITED STATES
DEPARTMENT OF ENERGY
(Pittsburgh Energy Technology Center)

Under Contract No. DE-FG22-86PC90526

PARTIAL OXIDATION OF LIGHT ALKANES

IN TRANSITION METAL ION CONTAINING ZEOLITES

SUMMARY OF PROGRESS

Fe(II)-A zeolites have been prepared, thermally pretreated, probed with specific adsorbing species such as CO and NO, and examined by diffuse reflectance spectroscopy as detailed in a previous quarterly progress report (DOE/PC/90526-7, June 1988). The spectral data have been further analyzed and the species that give rise to the spectral features are assigned and discussed. Some of the figures that were presented in the referenced report are given here to aid in the discussion.

Upon thermal dehydration, the Fe(II)-A zeolite exhibited consecutively hexaquo, monoaquo, and surface trigonal Fe^{2+} species. The adsorption of NO molecules proved the accessibility of the surface trigonal iron sites. Upon contact with O_2 at 700K, the ferrous ions were oxidized to ferric species. This process consumed about one oxygen atom per two iron ions. The oxidized Fe(II)-A zeolite could oxidize methane to water and carbon dioxide at temperatures as low as 600K. At the same time, a fraction of the back-reduced cations was converted to amorphous iron oxide, the presence of which conferred an enhanced activity for methane oxidation to the zeolite.

Extended Hückel calculations are being performed for several model clusters in an attempt to clarify the bonding scheme, the stability, and the electronic structure of these reactive ferrous complexes, particularly of the surface trigonal and the mononitrosyl Fe^{2+} species.

TECHNICAL PROGRESS

Characterization of Fe(II)-A Zeolite

The X-ray diffraction analyses of the starting Na-A and the exchanged Fe(II)-A samples gave similar powder patterns indicating that the zeolite structure was retained. Slight shifts at the peak positions toward higher angles were observed for the exchanged samples supporting a successful exchange. The X-ray diffraction peaks started to broaden upon heating the Fe-A zeolites in air at and above 700K as a result of collapse of the zeolite structure.

The zeolite used for most of the studies was a $Fe_{3.36}$-A zeolite, and atomic absorption analysis indicated 12.19 wt% Si, 11.88 wt% Al, 6.78 wt% Na, and 4.24 wt% Fe, corresponding to an ideal unit cell formula of $Fe_{3.36}Na_{5.10}H_{0.35}(AlO_2)_{12.14}(SiO_2)_{12.00}$.

Dehydration

The hydrated Fe(II)-A zeolite exhibited a pale green color. Its optical spectrum, recorded after dehydration by evacuating for 2 h at room temperature, showed two sharp vibrational bands for water, a combination band ($\nu + \delta$) at 5160 (±5) cm^{-1} and the first overtone band (2ν) at 6840 (±10) cm^{-1} [1], and weak broad bands corresponding to electronic transitions at 8400 (±140), 10,870 (±20) and 14,840 (±40) cm^{-1} (Figure 1, spectrum a). A similar spectrum was observed for the $FeSO_4.7H_2O$ salt, but the band at 14,840 cm^{-1} was significantly weaker compared to the two other ones. Upon outgassing at 300K and further up to 400K, all bands, including the vibration bands of water, decreased significantly in intensity, and a new large band formed at 5714 (±16) cm^{-1} (Figure 1, spectrum b). The residual $\nu + \delta$ water band shifted up to 5192 (±10) cm^{-1}. The 2ν band is about 5 times

less intense than the $\nu + \delta$ band, and it could no longer be detected. Upon dehydration at and above 450K, the spectral bands due to water vanished, indicating that the dehydration was completed. Meanwhile, the band at 5714 cm^{-1} was substituted by two intense and well resolved bands at 7936 (±12) and 9615 (±18) cm^{-1} (Figure 1, spectrum c). As the dehydration temperature increased a weak shoulder present at about 6000 cm^{-1}, and another band located at 13,000 cm^{-1}, decreased in intensity, and the base line increased as a consequence of the shift of the absorption edge toward lower energy. At 700K the zeolite had still a pale green, almost white, color. No longer was a significant water band detectable around 5200 cm^{-1}. Attention has been paid to the possible appearance of a hydroxyl band around 7300cm^{-1} at each dehydration step, but such a band was never detected. However, the low extinction coefficient of such a hydroxyl band, comparable to that of the 2ν water band, together with the presence of the strong absorption tail around 7300 cm^{-1} do not allow the complete exclusion of the presence of some OH groups due to partial hydrolysis of the cations.

Recorded at 600K, the spectrum of the fully dehydrated Fe-A zeolite exhibited the same two optical bands around 7950 and 9600 cm^{-1} (Figure 2), indicating that the cation coordination has not changed drastically at high temperature. It is worth noting that an A zeolite containing 0.5 Fe(II) cation per unit cell, indicated as $Fe_{0.5}$-A as opposed to the previous $Fe_{3.36}$-A, also exhibited comparable bands at 7936 and 9615 cm^{-1} in a comparable intensity ratio.

Adsorption of Probe Molecules

The adsorption of CH_4, CO and NO was followed by volumetric measurements and UV-VIS-NIR spectroscopy. At about 90 kPa pressure, methane adsorbed onto the Fe(II)-A zeolite ($Fe_{3.36}$-A) only up to 0.60 (±0.01)

molecule per unit cell, i.e. about 0.18 molecule per iron cation. The adsorption proceeded almost instantaneously, and no significant change in the optical spectrum of the zeolite was observed. Upon outgassing, 99% of the adsorbed methane was recovered.

Under 106 kPa of CO, the Fe(II)-A zeolite adsorbed 1.17 (±0.02) CO molecules per unit cell, i.e. about 0.35 molecule per iron cation. More than 93% of the adsorbed CO molecules could be desorbed under vacuum at room temperature. However, adsorbed CO interacted only weakly with the Fe^{2+} cations. The two optical bands at 7936 and 9615 cm^{-1} were only slightly affected by the CO adsorption (Figure 3). The initial spectrum was fully restored upon outgassing.

The NO adsorption has been performed on a sample that has been oxidized and subsequently reduced, and it also exhibited the two optical bands at 7936 and 9615 cm^{-1} (Figure 4, Spectrum a). A more detailed description of this spectrum will be provided in the next paragraph. Upon contact with NO at 53 kPa pressure, the zeolite instantaneously turned to dark green, and 1.91 (±0.05) NO molecules were adsorbed per unit cell, i.e. about 0.57 molecule per iron cation. The two bands at 7936 and 9615 cm^{-1} vanished, and two very intense bands developed around 15,000 and 22,000 cm^{-1}, on the tail of a strong absorption edge (Figure 4, Spectrum b). The weak band observed around 7000 cm^{-1} is possibly the shoulder that was present at 7000 cm^{-1} before the NO adsorption (Figure 4, spectrum a). The desorption of NO required heating above 500-550K. After heating gradually up to 700K, 84% of the NO could be desorbed. The bands at 15,000 and 22,000 cm^{-1} fully disappeared but the two optical bands of the dehydrated zeolite were recovered incompletely (Figure 4, Spectrum c). The powder exhibited a green-yellow color.

Redox Properties

At 100 kPa pressure and room temperature, oxygen adsorbed only up to 0.26 (±0.01) molecule per unit cell, or 0.08 O_2 molecule per Fe(II) ions. No change in the optical spectrum was observed. The adsorption was reversible within experimental error. As the temperature increased up to 700K, the amount of *immediately* adsorbed oxygen decreased below 0.05 molecules per unit cell. However, within several hours at 700K the extent of adsorption increased to about 0.75 (±0.05) oxygen molecule per unit cell, i.e. about 0.45 oxygen atom per iron cation. The sample became intense tan, and the two optical bands at 7936 and 9615 cm^{-1} completely disappeared (Figure 5, spectrum b). At the same time, the energy of the absorption edge was lowered from about 26,000 cm^{-1} down to about 18,000 cm^{-1}, giving rise to the tan color.

The initial spectrum could not be restored upon outgassing at 700K over night. However, it was partially recovered after reaction with methane at 700K and 100 kPa pressure for several days, the sample color changing from tan to gray. This treatment resulted in the appearance of a shoulder around 7000 cm^{-1} in the optical spectrum (Figure 5, spectrum c). The relative intensity of the shoulder increased as the number of oxidation-reduction cycles increased (Figures 5c and 5d). Meanwhile, the oxidation of the sample occurred somewhat more easily after several redox cycles. A similar reduction has been observed upon reduction of the oxidized $Fe_{0.5}$-A with H_2 and CO at 600K or with CH_4 at 700K.

Methane Oxidation

The initial activity of the oxidized Fe(II)-A zeolite was first investigated by keeping the methane conversion low in order to minimize the

number of oxidized cations to be reduced. At and above 600K, under 120 kPa of pure methane, an increase in the partial pressure of CO_2 was observed. The higher the temperature, the greater was the formation of CO_2 (Figure 6). Surprisingly, no increase in the H_2 or H_2O partial pressure was observed, as expected from a material balance point-of-view. The pressure of methane decreased monotonously, mainly due to the leak valve open to the mass spectrometer. No component partial pressure other than CO_2 was found to increase as the reaction performed. The apparent induction period in the formation of CO_2 was probably not due to reaction kinetics but rather to secondary effects like adsorption on the walls of the vacuum line. Indeed, a much larger induction period occurred when the reaction proceeded with the vacuum line at room temperature rather than at 400-420K.

In an additional experiment, the zeolite was subjected to five redox cycles, involving typically 24 h of oxidation at 700K and 100 kPa pressure of pure O_2 followed by 24 h up to 6 days of reduction at 700K and ≈100 kPa pressure of pure methane. After the last oxidation step, the methane reacted to form CO_2 at a rate about 2 times faster than previously. Moreover, a small increase, i.e. 1% and 4% of the CO_2 increase, was observed at the highest conversions for mass 18 (water) and mass 28 (carbon monoxide), respectively. Hence, some water was formed in the reaction. The increase in mass 28 was most probably due to fragmentation of the CO_2. No other mass smaller than 100 was ever found to increase during the reaction. Supporting further the conclusion that water was formed, the background level of water was found to increase significantly when the zeolite was outgassed at 700K after the reaction with methane.

The possibility of carbon deposition in the zeolite during the methane oxidation was investigated by calcining the sample at 700K and 100 kPa

pressure of pure O_2 after having outgassed the catalyst and purged it with N_2 for few hours at the same temperature. No CO_2 formation was detected within 90 min, although the zeolite color turned back to tan indicating the oxidation of the ferrous ions into their ferric form. Hence, no coke had been deposited.

Finally, the reaction of methane with the reduced catalyst has also been investigated. Even at temperatures as high as as 700K, the adsorption of methane was almost negligible and did not induce any change on the optical spectrum of the Fe(II)-A zeolite. After a 7 h run at 700K and 120 kPa pressure of CH_4, only 0.8% CO_2 was detected compared to 12% formed over the oxidized catalyst. Hence, the reduced form of the Fe-A zeolite was inactive for the methane oxidation.

DISCUSSION

Depending on the extend of dehydration, which was monitored by the NIR bands due to water, the Fe(II)-A zeolite exhibited different optical spectra. They corresponded to hydrated, partially hydrated, and fully dehydrated Fe(II) species. Those species will be identified in the following paragraphes.

Hydrated Fe(II)-Species

When largely hydrated, as indicated by the strong NIR vibrational water bands, the Fe(II)-A zeolite exhibited two weak electronic transitions at 8400 and 10,870 cm^{-1}. Similar transitions were observed for the $FeSO_4.7H_2O$ salt used in the cation exchange, as well as for aqueous Fe^{2+} solutions [2]. They are widely recognized as being due to the $^5T_2 \rightarrow {}^5E$ transition of the high-spin octahedral $Fe(H_2O)_6^{2+}$ complex, with further Jahn-Teller splitting

in the excited ^5E state [2]. The presence of an inversion center in such complexes is then responsible for the small intensity of the d-d transitions, as observed in the present case. Hence, the Fe(II) in hydrated Fe(II)-A zeolite is octahedrally coordinated with 6 water molecules or possibly with 3 water molecules and three framework oxygens. This picture is consistent with the results of Mössbauer studies performed on several Fe(II) exchanged zeolites [3-7].

The third broad band observed at 14,840 cm^{-1} cannot be attributed to octahedral Fe(II), but its presence may indicate additional partially dehydrated cation species, e.g. one containing only two water molecules.

Partially Dehydrated Fe(II)-Species

The Fe(II)-A zeolite that was partially dehydrated at 400K exhibited a small vibrational band of residual water at 5300 cm^{-1} and a strong electronic band of the complex at 5714 cm^{-1} (Figure 1b). The strong intensity of the electronic transition indicated the disappearance of the inversion center for the d-d transitions. Since tetrahedral complexes have a splitting of the d-levels roughly equal to one-half of the splitting of the corresponding octahedral complexes, the transition observed at 5714 cm^{-1} most probably indicates Fe(II) ions in nearly tetrahedral coordination. Such a site would involve three framework oxygens and one residual water molecule, as it has been observed in partially dehydrated Ni(II)- and Co(II)-A zeolites [8,9]. This monoaquo complex is being investigated by extended Hückel calculations.

For a comparable state of dehydration of the Fe(II)-A zeolite, Dickson and Rees [6] observed a new Mössbauer doublet having a quadrupole splitting (QS) of 1.4 $mm \cdot s^{-1}$, i.e. intermediate between the splitting observed for the fully hydrated (QS = 2.1 $mm \cdot s^{-1}$) and the fully dehydrated (QS = 0.46 $mm \cdot s^{-1}$)

samples. They attributed this doublet to a partially hydrolyzed cation (Z-O)$_3$Fe^{2+}(H$_2$O)$_2$OH$^-$, where Z-O represents framework oxygens. The presence of a hydroxyl group cannot be ruled out by the present NIR studies. However, the monoaquo complex may also account for the QS = 0.46 mm·s^{-1} of the new Mössbauer doublet.

Dehydrated Fe(II)-Species

Once the Fe(II)-A zeolite was fully dehydrated, as indicated by the absence of vibrational NIR water bands, it exhibited well-resolved, relatively intense electronic transitions at 7936 and 9615 cm^{-1} (Figure 1c). The large intensity of the bands indicated again the absence of an inversion center for the d-d transitions. It should first be recognized that the presence of two optical bands is not due to the presence of two different cation sites. If that were the case, one of the two sites would be preferentially occupied at lower iron loading, resulting in the appearance of a single transition. However, the 7936-9615 cm^{-1} doublet was also observed for an Fe(II)-A zeolite that contained only 0.5 iron cation per unit cell.

The dehydrated Fe(II)-A zeolite was reported to contain an accessible trigonal Fe(II) ion that was characterized by a specific Mössbauer doublet [6]. However, an identical Mössbauer doublet, observed by other researchers in Fe(II)-Y zeolite [10], was instead attributed to a more hidden tetrahedral-like four-fold coordinated Fe(II) because of its low accessibility for probe molecules. The four-fold coordination of the Fe(II) could be ruled out in the present case. First, the ions were highly accessible for NO molecules. Second, nearly tetrahedral complexes are characterized by electronic transitions at energies smaller than 8000 to

9000 cm^{-1}, as discussed earlier for the monoaquo complex. Hence, the dehydrated Fe(II) species are conclusively in a trigonal coordination similar to that observed by X-ray diffraction studies for other divalent cations exchanged in A-type zeolites (e.g. [11]).

The ligand field interpretation of the optical transition of such a bare trigonal site is very sensitive to the choice of the ligand field parameters G_2 and G_4 that represent the dipole and quadrupole ligand field strength, respectively [12,13]. This is illustrated well by comparing the interpretation of the optical spectrum of Cu(II)-Y zeolite performed by Strome and Klier [14] and Packet and Schoonheydt [15]. Depending on the value chosen for the G_2/G_4 parameter, a different ordering of the energy states was calculated: the energy increased in the order of $^2A'_1 < ^2E'' < ^2E'$ for G_2/G_4 between 5 and 10 [14] but in the order of $^2E'' < ^2A'_1 < ^2E'$ for G_2/G_4 below 2 [15]. The G_2/G_4 value increases with the ratio of the radius of the center-of-weight of the ligand electron distribution to the radius of the 3d electron distribution on the metal ion. The G_2/G_4 ratio also has an MO interpretation, utilized in Ref. 12, which favors low values of the ligand-Cu^{2+} ion bonding of σ-type and a high value if that bonding is of π-type. Packet and Schoonheydt argue in favor of the former, but the issue cannot be resolved by optical assignments only and for a single cation. At any rate, the G_2/G_4 ratios of 1.5 [15] and 10 [14] represent extremes for strong and weak oxygen-Cu^{2+} bonding, and the Fe^{2+} zeolite spectra will be discussed for both extremes.

The D_{3h} term diagrams calculated for the d^6 Fe^{2+} ion for $G_2/G_4 = 1.5$ and $G_2/G_4 = 10$ are presented in Figures 7a and 7b, respectively. Here also the ordering of the A_1' and E" states was reversed by the G_2/G_4 value. The term diagrams predict that only the higher of the two transitions will be

observed in the range of energies investigated, i.e. above 5000 cm^{-1}. For high G_2/G_4 values (Figure 7b), this transition would be $^5A_1 \rightarrow {}^5E'$ while for low G_2/G_4 values (Figure 7a) it would be $^5E'' \rightarrow {}^5E'$. Two peaks are observed (Figure 1c) and, consistent with the earlier interpretation for Cu^{2+}, they are attributed to transitions into the Jahn-Teller-split excited $^5E'$ state. The amount of J-T splitting is 1620 cm^{-1}, which is comparable to the values of 1800 cm^{-1} [14] or 2200 cm^{-1} [15] reported for Cu^{2+}. By fitting of the d^6 term diagrams using the middle transition energy of 8775 cm^{-1}, the G_4 quadrupolar ligand field strength parameter was estimated to be $g_4 \approx 7240$ cm^{-1} in the case of low G_2/G_4 and $G_4 \approx 1040$ cm^{-1} in the case of high G_2/G_4. Indeed, G_4 is consistently calculated below 2500 cm^{-1} for Cr^{2+}, Fe^{2+}, Co^{2+}, Ni^{2+} and Cu^{2+} ions in the trigonal zeolite site when using high G_2/G_4. However, G_4 values above 5300 cm^{-1}, as obtained here by using a low value for G_2/G_4, are usually found for tetrahedral and octahedral coordinations. Hence, the low G_2/G_4 value proposed by Packet and Schoonheydt [15] seems to give a more uniform representation of the ligand field splitting in various coordination geometries. This conclusion is being probed by the extended Hückel calculations that are being carried out.

Water in Hydrated and Partially Dehydrated Fe(II)-A Zeolites

The intensity of the vibrational $\nu + \delta$ combination band of water (as defined in [1]) observed in the fully and partially hydrated samples was used to estimate the water content. Klier et al. [1] presented the relation between the intensity of the H_2O ($\nu + \delta$) band and adsorbed amounts of water in Na-A zeolite. Since the samples and the diffuse reflectance cells used in both studies were similar, the results were expected to be comparable. Using a calibration curve of Klier et al. (Figure 8), the intensity of the water ($\nu + \delta$) band indicated the presence of 16-18 water molecules per unit

cell in the fully hydrated sample and 7-8 molecules per unit cell in the partially hydrated sample. This corresponds to about five and two molecules of water per iron ion, respectively. In the hydrated zeolite, a large fraction of the Fe^{2+} ions could have been in the form of a hexaquo complex, with only a small number coordinated with three framework oxygens and three (or less) water molecules. It is noted here that the frequency of the water band in the hydrated sample was lower than that observed for bulk water or fully hydrated Na-A zeolite [1], namely 5160 instead of 5190 cm^{-1}. This indicates that a large number of the water molecules were indeed coordinated to the iron cations and, consequently, the OH band frequency was lowered. In the case of partially hydrated zeolite, the observed electronic transition indicated the presence of a monoaquo Fe-complex, i.e. of one water molecule per iron ion, but the water (ν + δ) band indicated the presence of two water molecules per Fe cation. Such an excess of tightly bonded water can be attributed to the encapsulation of water molecules in the sodalite cages [16,17].

Adsorption of Probe Molecules

Two observations indicated that the CO and CH_4 adsorption were rather weak: (i) the CO or CH_4 adsorption did not induce major changes in the optical spectrum of iron, and (ii) CO and CH_4 were easily desorbed by outgassing at room temperature. In any case, the weak adsorption of CO or CH_4 did not permit the conclusion that the iron ions were poorly accessible. By considering the NO adsorption on Fe(II)-A zeolite, it was evident that the trigonally coordinated Fe^{2+} cations were highly accessible, as indicated by the instantaneous adsorption of NO followed by the disappearance of the two optical bands at 7936 and 9615 cm^{-1}. In addition, the nitrosyl complex

was very stable, as evidenced by the high temperature required to desorbe NO and restore the optical bands at 7936 and 9615 cm^{-1}.

Jermyn et al. [18], as well as Dumesic et al. [19,20], reported that a similar Fe^{2+} site in Fe(II)-Y zeolite, i.e. the trigonally coordinated SII or SII' Fe^{2+} ion, adsorbed NO to form a strong, mononitrosyl complex. Hence, the stoichiometry of 0.57 NO molecule per iron ion observed in the current study most probably indicates that about 43% of the cations were inaccessible because of amorphous iron oxide that was present before the NO adsorption (see shoulder around 7000 cm^{-1} in spectra a and b in Figure 4). The spectroscopic study of Jermyn et al. [18] gave further information on the mononitrosyl complex formed on the SII or SII' site in Fe(II)-Y zeolite. First, the EPR results revealed a spin state of S = 3/2, indicating the pairing of the π^* NO electron with a 3d iron electron to form either an $[Fe(III)\text{-}NO]^{2+}$ or $[Fe(I)\text{-}NO]^{2+}$ complex [18]. Second, the IR investigations showed a relatively high frequency for the NO stretching vibration, i.e. 1890 cm^{-1} [18] or 1870 cm^{-1} [19] instead of 1840 cm^{-1} for gaseous molecules. This favored the $[Fe(I)\text{-}NO]^{2+}$ complex by indicating a decrease of the population of the antibonding π^* orbital of NO [18].

Consistent with the observations of Jermyn et al. [18], the optical spectrum reported here for the nitrosyl complex (Figure 4b) indicated a complete change of the electronic structure of the Fe^{2+} ion. The cation was neither planar trigonal Fe^{2+}, because of the disappearance of the bands at 7936 and 9615 cm^{-1}, nor tetrahedral-like Fe^{2+}, because of the absence of a band around 5000-6000 cm^{-1}. The bands that developed at 15,000 and 22,000 cm^{-1} had an intensity too large to be attributed to d-d transitions and must indicate charge transfer transitions. However, the UV-VIS-NIR results did not provide for differentiating between the Fe(I) and Fe(III) species.

Redox Properties

The trigonally coordinated Fe^{2+} ions were accessible to gaseous molecules by adsorbing NO. However, no significant O_2 adsorption was observed at room temperature, in contrast to Cr^{2+} for which a reversible dioxygen [$Cr(III)\text{-}O_2^-$] complex was formed under similar conditions [21]. Klier et al. calculated the relative one-electron oxidation potentials (termed "oxidizabilities") of the M^{2+} 3d-cations by correcting their third atomic oxidation potential with the change in crystal field stabilization energy that the cations undergo changing from trigonal to tetrahedral coordination [13]. The resulting series of oxidation potentials was predicted to be

$$Sc^{2+}<Ti^{2+}<V^{2+}<Cr^{2+}<Fe^{2+}<Mn^{2+}<Co^{2+}<Ni^{2+}<Cu^{2+}<Zn^{2+},$$

and this followed the order of increasing atomic mass except for an inversion in the positions of Fe^{2+} and Mn^{2+} due to the stability of the half-filled shell of the Fe^{3+} product. Since a dioxygen complex was reported for Cr^{2+} but not for Co^{2+} [9] or for Fe^{2+}, one can determine the minimum relative "oxidizability" required for the formation of a dioxygen complex to be between -31.8 eV (for Cr^{2+}) and -32.2 eV (for Fe^{2+}).

The Cr^{2+}-A zeolite was reported to form also an irreversible monoxygen [$Cr(IV)\text{-}O^{2-}$] complex at elevated temperatures, e.g. 420K [21]. For the irreversible oxidation of Fe(II)-A, however, much higher temperatures were required, indicating a higher activation energy. The Fe(II)A-oxygen complex differed from the chromium complex by two aspects: the final oxidation state of the cation and the oxygen-cation stoichiometry. First, the Fe cation ended up in its third oxidation state, as already reported from Mössbauer studies of Fe-Y zeolite, Fe-mordenite, and Fe-A zeolite [5,10,22]. Indeed, the optical spectrum of the oxidized Fe(II)-A zeolite exhibited only

a broad and strong charge transfer band above 18,000 cm^{-1} but no bands due to the d-d transitions at lower frequencies. This is consistent with a high spin d^5 ion that only has spin forbidden electronic transitions. The charge transfer band was probably due to electronic transitions between the 2p levels of the neighboring oxygen ligands and the 3d levels of iron. The low energy observed for the oxygen-Fe(III) charge transfer transition is typical of ferric oxide [23]. It can be explained by considering a stabilization of the iron 3d levels due to the increased nuclear charge and the decreased repulsion among the 3d electrons in Fe(III) compared to Fe(II). The second difference with the irreversible chromium-oxygen complex was that the irreversible Fe-oxygen complex did not form according to the stoichiometry of one oxygen atom per Fe cation, as in the case of Cr(II)-A, but rather one oxygen atom per two iron cations. This stoichiometry was previously observed in the case of Fe(II)-Y [10] and Fe(II)-mordenite [5]. The requirement of an Fe pair in close proximity for the oxidation on Fe(II)-Y zeolite was previously indicated by the facts that (i) the Fe(II)-exchanged silicon framework-substituted type-Y zeolite, which had a relatively low Fe loading, was more difficult to oxidize than the conventional cation-exchanged Fe-Y [24], and (ii) the magnetic moment of 4.4 Bohr magnetons observed in oxidized Fe(II)-Y zeolite, being lower than the spin-only magnetic moment of the Fe(III) ions at 5.9 Bohr magnetons, could indicate anti-parallel spin coupling interactions between the Fe(III) ions via superexchange [25]. All these results support the reaction stoichiometry:

$$2Fe^{2+} + 1/2O_2 \rightarrow 2Fe^{3+} + O^{2-}.$$

This stoichiometry possibly indicates that this O^{2-} species is bound to two iron cations forming an Fe(III)-O^{2-}-Fe(III) bridge, as proposed by Garten et al. [10]. The presence of such a bridge has been rejected by Pearce et al.

using powder X-ray diffraction of Fe-Y zeolites [26]. The conditions used by Pearce et al. [26] seem, however, not to be comparable with those of Garten et al. [10] and those employed in the present study, as indicated by the fact that Pearce et al. [26] observed an exceptionally large loss of zeolite crystallinity upon redox treatment.

The Fe cations did not undergo redox cycles with complete reversibility and a new shoulder developed around 7000 cm^{-1}, indicating some amorphous iron oxide, e.g. in distorted tetrahedral coordination. This partial irreversibility, already observed by Mössbauer studies of Fe(II)-Y [26] and Fe(II)-A zeolite [22], has been attributed to the presence of water during the oxidation steps [27].

Methane Oxidation

The methane reaction experiments showed that the oxidized Fe(II)-A zeolite can activate methane under relatively mild conditions, namely at atmospheric pressure and 600 K. Under these conditions, methane was fully oxidized to CO_2 and H_2O. Gaseous water was not readily detected and was apparently retained by the zeolite. Since only a small fraction of the cations was reduced, the water concentration retained by the zeolite was probably very low and, therefore, could not be detected spectroscopically in the NIR. The experimental conditions were such that it is not surprising to observe a full oxidation since a batch reactor and a small pore zeolite were used and a fairly high concentration of iron per unit cell implies a large residence time of methane on the active sites.

Because the reduced zeolite was found to be inactive for the methane oxidation in the absence of oxygen, the active sites should involve the oxygen/ferric-ion complex. As shown by the oxidation experiments and the

optical studies, the application of several redox treatments resulted in an increase in oxidation activity together with formation of amorphous iron oxide due to a loss in the zeolite crystallinity. Furthermore, it rendered the zeolite more readily oxidizable. Similar observations, reported mainly by Boreskov as reviewed by Maxwell [28], have already been made for the oxidation of carbon monoxide on Cr(III)-, Fe(II)-, Co(II)-, Ni(II)- and Cu(I)-X and Y zeolites. An increase in oxidation rate was reported with excessive cation loading or pH of the exchange medium. The enhanced activity of the bridged chemisorbed oxygen M^{n+}-O^{2-}-M^{n+} was attributed to the higher covalency of its bonding to the metal ions.

The complete oxidation of methane has been performed by Rudham and Sanders over Fe(III) exchanged X-type zeolite under a CH_4/O_2 flow [29]. Although the experimental conditions were different than here, particularly the preparation of the catalyst by exchange with Fe(III) [32] instead of Fe(II), a similar reactivity was reported in both cases. Since the Fe(III)-X zeolite is known to undergo partial cation reduction to Fe(II) upon dehydration [3], it is probable that the oxidation reaction reported by Rudham and Sanders [29] proceeded on oxygen species that were chemisorbed on the oxidizable Fe(II) cations that appeared upon dehydration. However, it cannot be ruled out that the reaction consumed lattice oxygen, reducing consequently Fe(III) to Fe(II), with the oxidation step being required to reoxidize Fe(II) and regenerate the lattice oxygen. Both mechanisms would be consistent with the zero reaction order with respect to oxygen observed by Rudham and Sanders [29].

CONCLUSIONS

The present optical study of the dehydration, the adsorption of probe molecules, and the redox behavior of Fe(II)-A zeolite led to the following conclusions:

1. Upon dehydration the Fe(II) species transformed from an octahedral hexaquo complex via a tetrahedral monoaquo complex to a nearly planar trigonal Fe(II)-site.
2. CH_4, CO, and O_2 did not interact with the trigonal Fe(II)-site at room temperature. The lack of O_2 adsorption allowed an estimate of the minimum 'relative oxidizability' required for the formation of a dioxygen complex.
3. NO was strongly adsorbed on the trigonal Fe(II)-site forming a mononitrosyl complex. NO was desorbed only at high temperature.
4. Fe(II) ions could be oxidized to Fe(III) by O_2 at 700K and then reduced back by CH_4 at 600K. However, some of the iron ended up in the form of amorphous oxide upon redox treatments.
5. The total oxidation of methane performed on the oxidized iron site in Fe(II)-A zeolite. No carbon was deposited. The activity of the zeolite was increased upon redox treatment, due probably to the presence of amorphous iron oxide.
6. A weak adsorption on Fe(II) cations was predicted for CO, while a strong one was estimated for NO. The stability of the nitrosyl complex was attributed to a partial electron transfer from the antibonding π^* NO orbital to the iron 3d orbitals and the consequent increase in N-O bond strength.

7. Estimates were made for the ligand field parameters G_2 and G_4, and these supported the use of a low G_2/G_4 value for the interpretation of the optical spectrum of trigonally coordinated transition-metal ions in zeolites.

REFERENCES

1. Klier, K., Shen, J.H. and Zettlemoyer, A.C., Preprints, Div. Pet. Chem., ACS, 53 (1973).

2. Greenwood, N.W. and Earnshaw, A., "Chemistry of the Elements", p. 1270, Pergamon Press (1984).

3. Morice, J.A. and Rees, L.V.C., Trans. Faraday Soc., 64, 1388 (1968).

4. Delgass, W.N., Garten, R.L. and Boudart, M., J. Phys. Chem., 73, 2970 (1969).

5. Garten, R.L., Gallord-Nechtschein, J. and Boudart, M., Ind. Eng. Chem. Fundam., 12, 299 (1973).

6. Dickson, B.L. and Rees, L.V.C., J. Chem. Soc., Faraday I, 70, 2038 (1974).

7. Fitch, F.R. and Rees, L.V.C., Zeolites, 2, 33 (1982).

8. Klier, K. and Ralek, M., J. Phys. Chem. Solids, 29, 951 (1968).

9. Klier, K., Adv. Chem. Series, 101, 480 (1971).

10. Garten, R.L., Delgass, W.N. and Boudart, M., J. Catal., 18, 90 (1970).

11. Seff, K., Acc. Chem. Res., 121 (1976).

12. Kellerman, R. and Klier, K., in "Surface and Defect Properties of Solids", Vol. 4 (M.W. Roberts and J.M. Thomas, eds.), p. 1, Chem. Soc. London (1975).

13. Klier, K., Hutta, P.J. and Kellerman, R., ACS Symp. Ser., 40, 108 (1977).

14. Strome, D.H. and Klier, K., ACS Symp. Ser., 135, 155 (1980).

15. Packet, D. and Schoonheydt, R., ACS Symp. Ser., 398, 203 (1988).

16. Shen, J.H., Zettlemoyer, A.C. and Klier, K., J. Phys. Chem., 84, 1453 (1980).

17. Breck, D.W., "Zeolite Molecular Sieves", pp. 133 & 427-430, Wiley, New York (1984).

18. Jermyn, J.W., Johnson, T.J., Vansant, E.F. and Lunsford, J.H., J. Phys. Chem., 77, 2964 (1973).

19. Segawa, K.-I., Chen, Y., Kubsh, J.E., Delgass, W.N., Dumesic, J.A. and Hall, W.K., J. Catal., 76, 112 (1982).

20. Aparicio, L.M., Hall, W.K., Fang, S.-H., Huppa, M.A., Millman, W.S. and Dumesic, J.A., J. Catal., 108, 233 (1987).

21. Kellerman, R. and Klier, K., ACS Symp. Ser., 40, 120 (1977).

22. Gao, Z. and Rees, L.V.C., Zeolites, 2, 215 (1982).

23. See Reference [2], p. 1265.

24. Aparicio, L.M., Dumesic, J.A., Fang, S.-M., Long, M.A., Ulla, M.A., Millman, W.S. and Hall, W.K., J. Catal., 104, 381 (1987).

25. Aparicio, L.M., Ulla, M.A., Millman, W.S. and Dumesic, J.A., J. Catal., 110, 330 (1988).

26. Pearce, J.R., Mortier, W.J. and Uytterhoeven, J.B., J. Chem. Soc., Faraday Trans. I, 77, 937 (1981).

27. Petunchi, J.O., Xu, Q.-H. and Hall, W.K., J. Catal., 84, 261 (1983).

28. Maxwell, I.E., Adv. Catal., 31, 1 (1982).

29. Rudham, R. and Sanders, M.K., J. Catal., 27, 287 (1972).

FIGURES

Figure 1. UV-VIS-NIR diffuse reflectance spectra of the dehydration of Fe(II)-A zeolite: (a) hydrated zeolite, (b) after partial dehydration at 400K, and (c) after full dehydration at 700K.

Figure 2. UV-VIS-NIR diffuse reflectance spectrum of dehydrated Fe(II)-A zeolite, recorded at 600K (the high background is due to a 50% loss of scattered light because of geometric factors).

Figure 3. UV-VIS-NIR diffuse reflectance spectra of the CO adsorption on Fe(II)-A zeolite: (a) before and (b) after adsorption.

Figure 4. UV-VIS-NIR diffuse reflecftance spectra of NO adsorption on reduced Fe(II)-A: (a) before and (b) after adsorption at 300K, (c) after desorption at 700K.

Figure 5. UV-VIS-NIR diffuse reflectance spectra of the oxidation and reduction of Fe(II)-A zeolite at 700K: (a) before and (b) after oxidation with O_2, and after (c) 3 and (d) 7 oxidation/reduction cycles with O_2 and CH_4.

Figure 6. CO_2 formation upon methane oxidation over pre-oxidized Fe(II)-A zeolite.

Figure 7. Term diagrams calculated for d^6 ion in D_{3h} symmetry using a G_2/G_4 of 1.5 (a) and 10 (b).

Figure 8. Calibration curve for the $\nu + \delta$ water band from hydrated Na-A zeolite (data from Reference [1]).

FIGURE 1

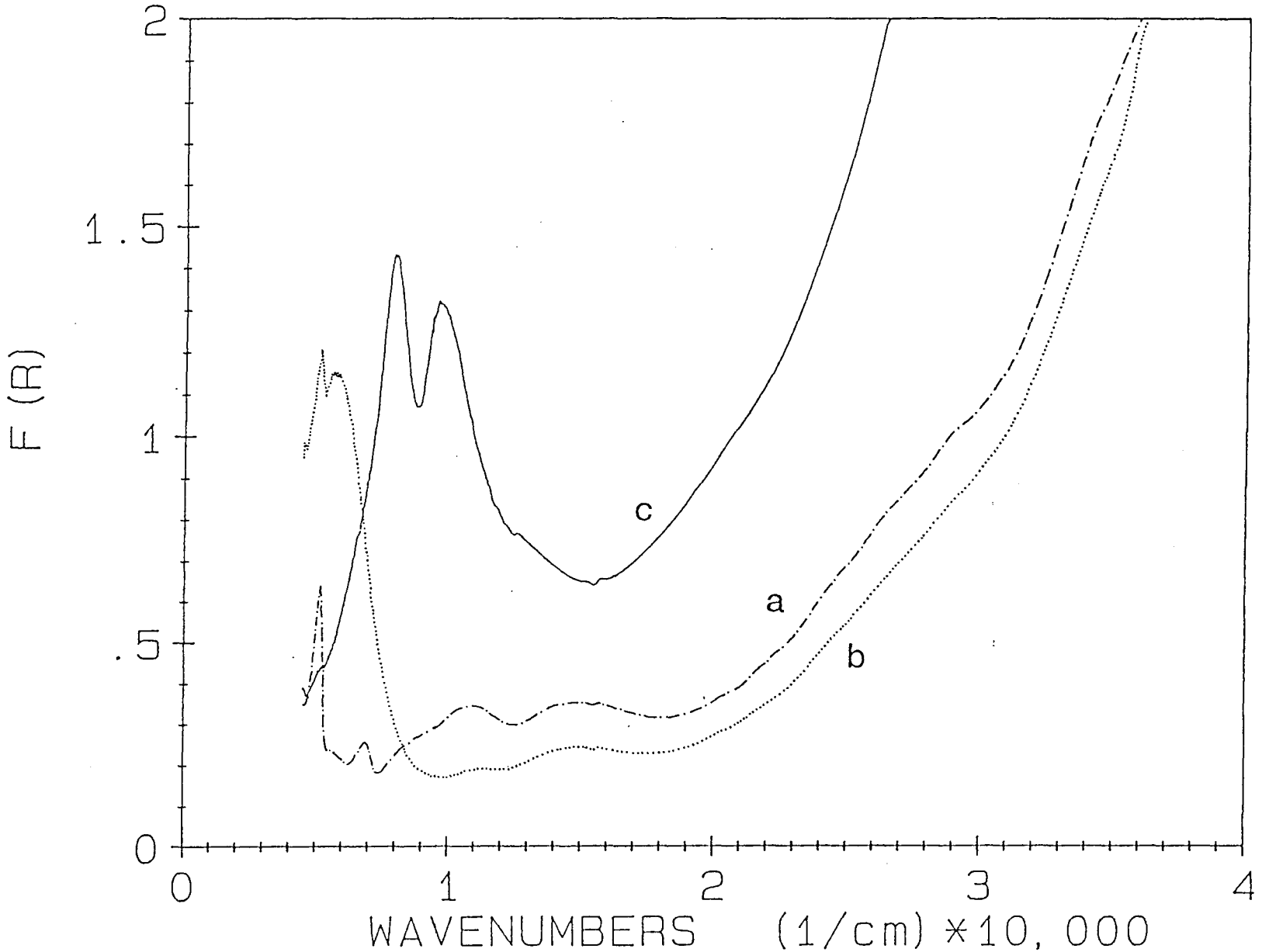

FIGURE 2

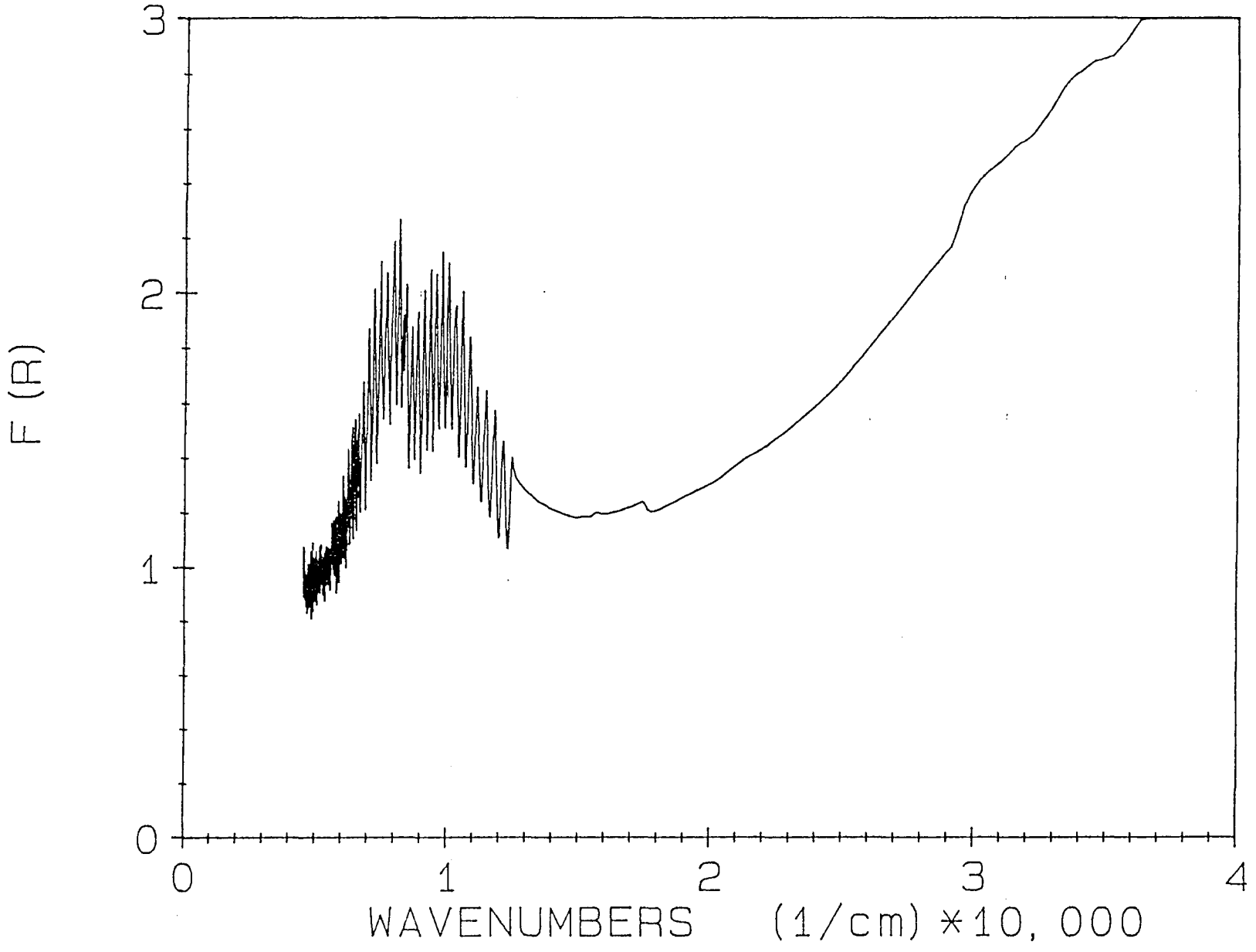

FIGURE 3

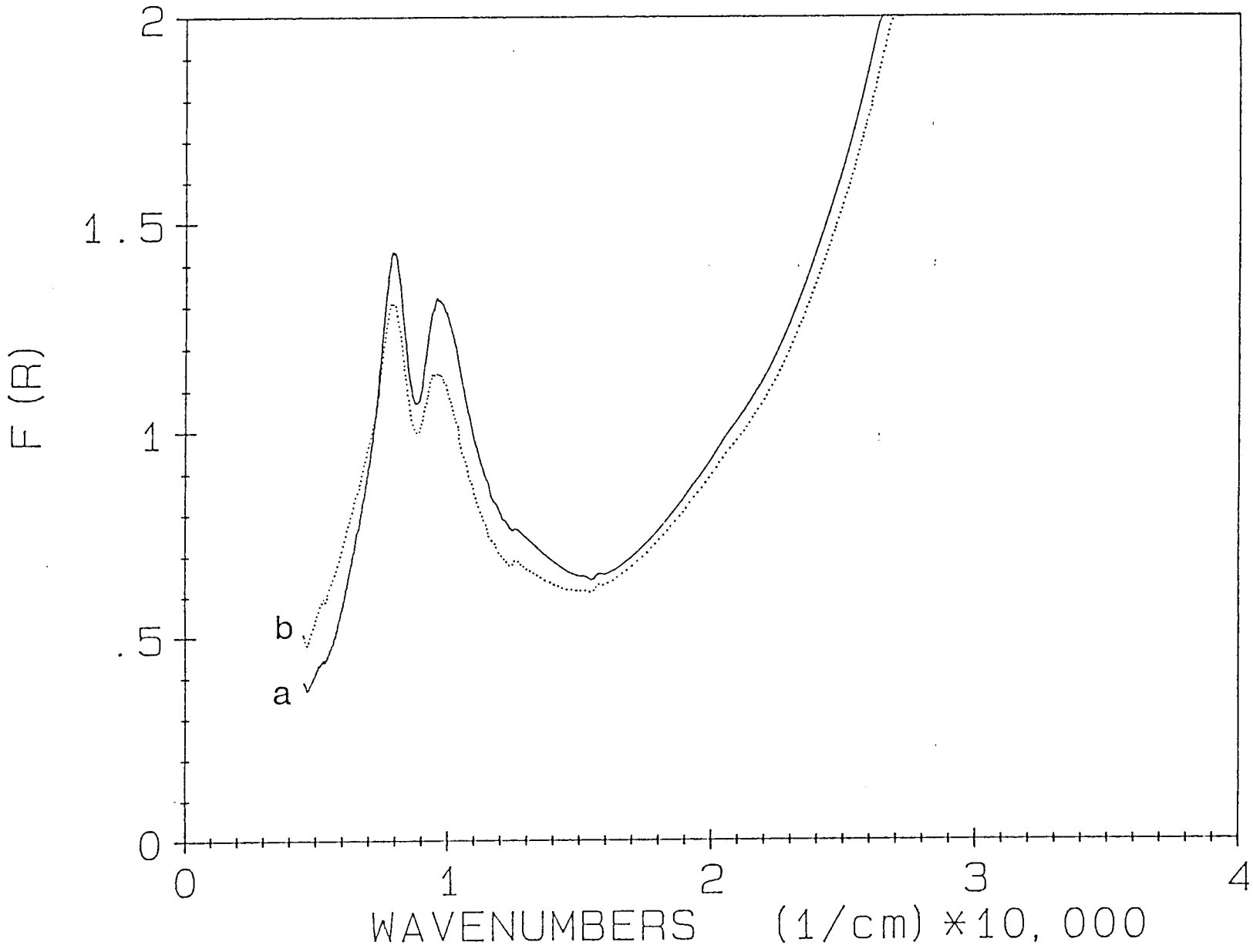

FIGURE 4

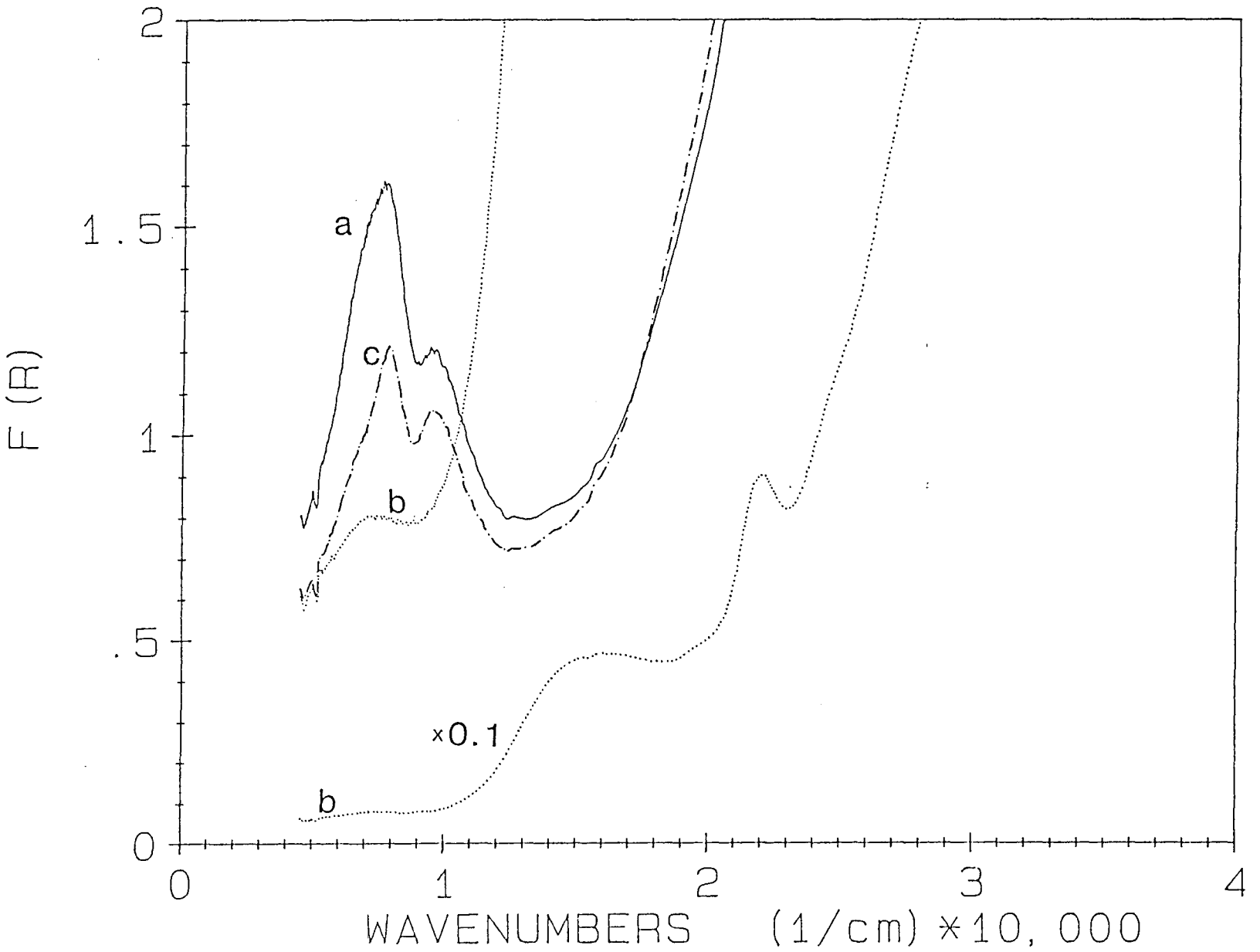

FIGURE 5

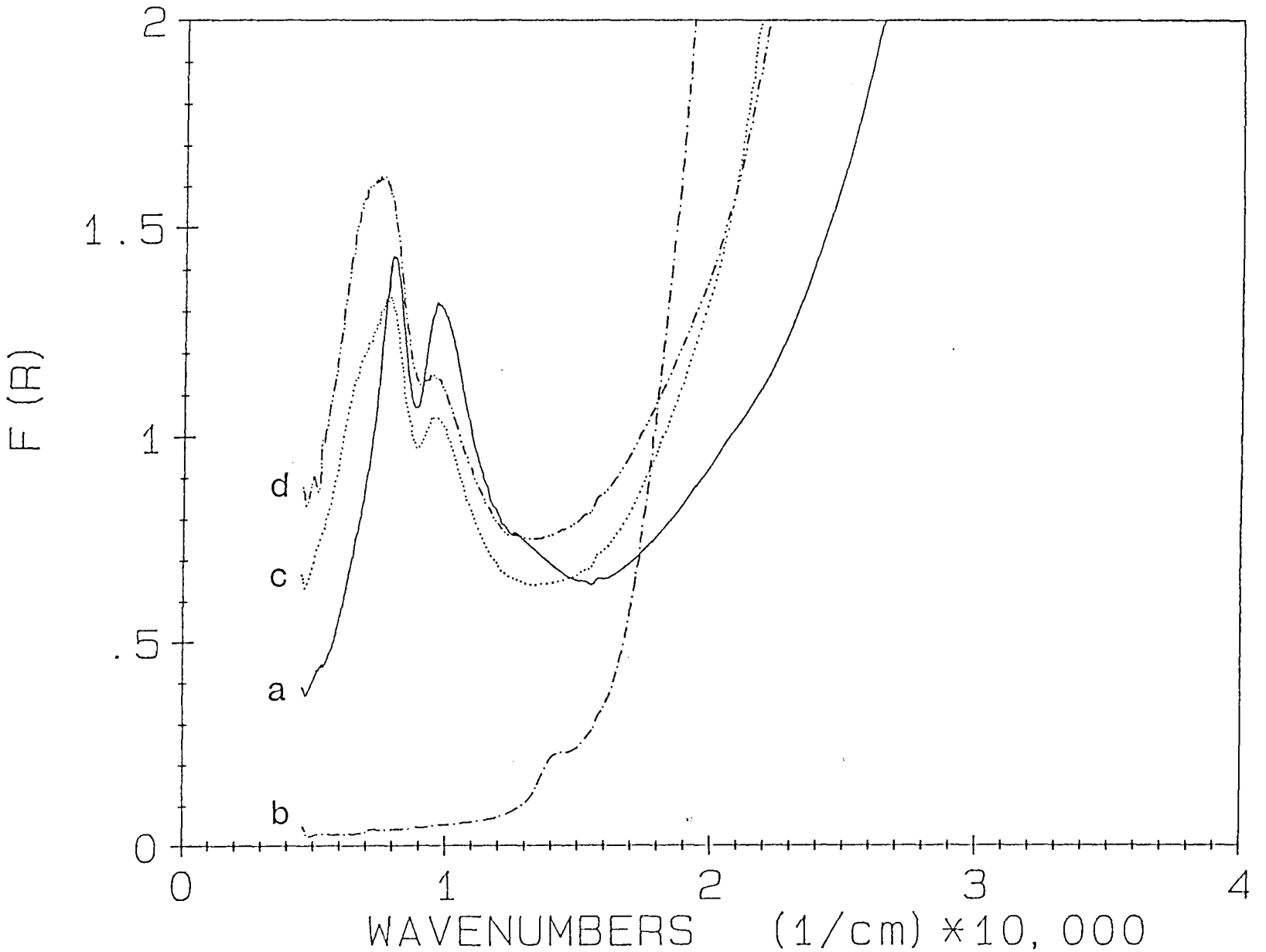

FIGURE 6

CH_4 OXIDATION OVER Fe(II)-A

Initial CO_2 Formation

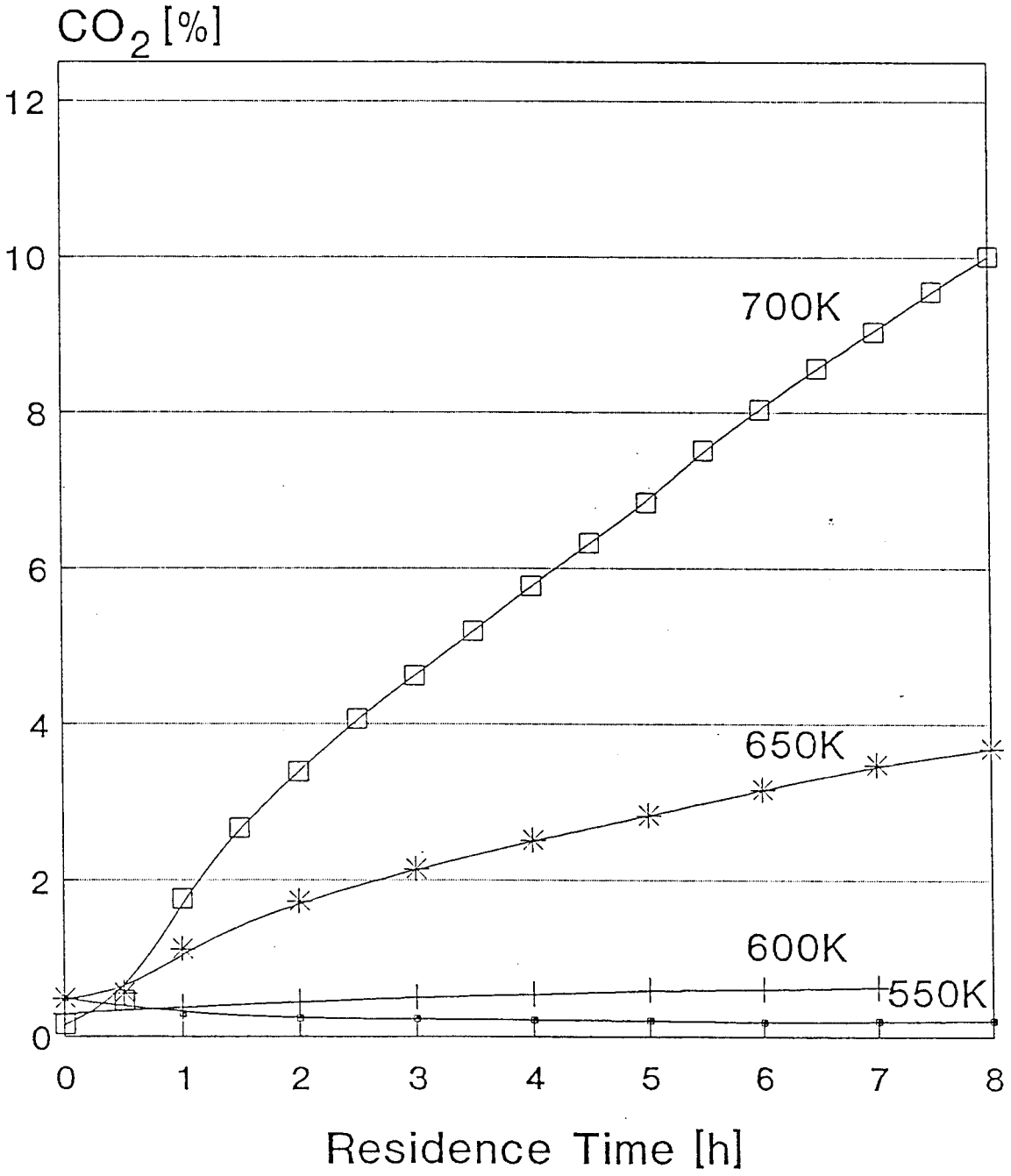

FIGURE 7

a

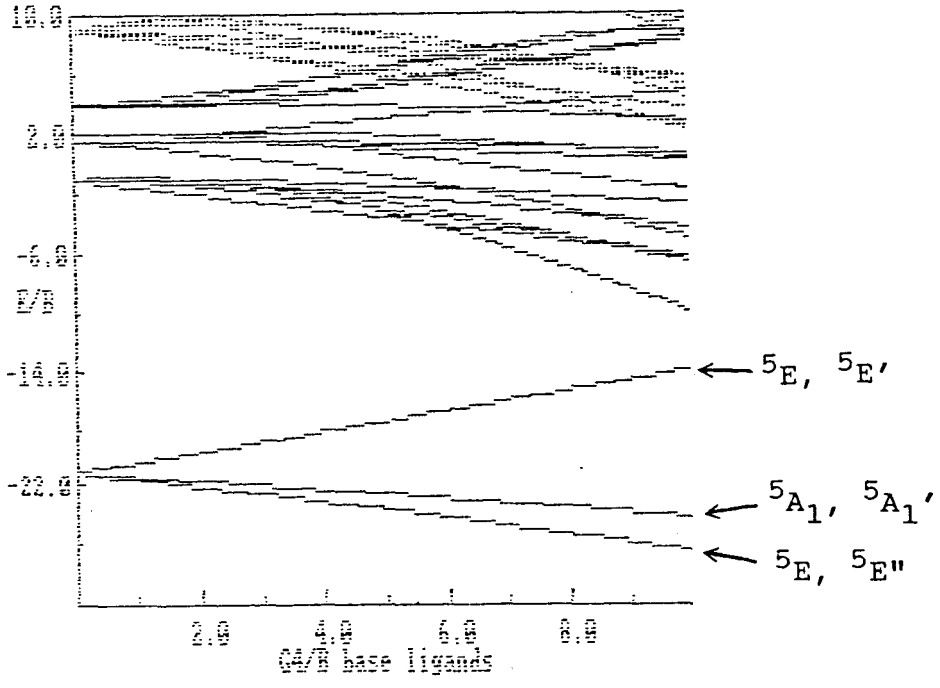
10.0
2.0
-6.0
E/B
-14.0
-22.0
2.0
4.0
6.0
8.0
Dq/B base ligands
^5E, $^5E'$
$^5A_1$, $^5A_1'$
^5E, $^5E''$

b

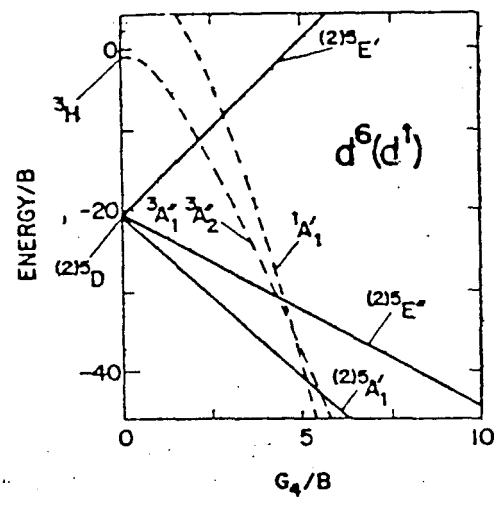
0
-20
-40
ENERGY/B
^3H
$(2)^5D$
$(2)^5E'$
$d^6(d^1)$
$^3A_1'$ $^3A_2'$
$^1A_1'$
$(2)^5E''$
$(2)^5A_1'$
0
5
10
G_4/B

FIGURE 8

CALIBRATION CURVE FOR THE NIR WATER BAND